Precise Modeling of the Exoplanet Host Star and CoRoT Main Target HD 52265

M. E. Escobar[1], S. Théado[1], S. Vauclair[1,2], J. Ballot[1], S. Charpinet[1], N. Dolez[1], A. Hui-Bon-Hoa[1], G. Vauclair[1], L. Gizon[3,4], S. Mathur[5], P.O. Quirion[6], T. Stahn[4]

[1] Institut de Recherche en Astrophysique et Planétologie, Observatoire Midi-Pyrénées, CNRS, Université Paul Sabatier, 14 Avenue Edouard Belin, 31400 Toulouse, France.
[2] Institut universitaire de France, 103 boulevard Saint Michel, 75005 Paris, France
[3] Max-Planck-Institut für Sonnensystemforschung, Max-Planck-Str. 2, 37191 Katlenburg-Lindau, Germany
[4] Institut für Astrophysik, Georg-August-Universität Göttingen, Friedrich-Hundt-Platz 1, 37077 Göttingen Germany
[5] High Altitude Observatory, NCAR, P.O. Box 3000, Boulder, CO 80307, USA
[6] Canadian Space Agency, 6767 Boulevard de l'Aroport, Saint-Hubert, QC, J3Y 8Y9, Canada
e-mail: mescobar@irap.omp.eu

ABSTRACT

Aims. This paper presents a detailed and precise study of the characteristics of the Exoplanet Host Star and CoRoT main target HD 52265, as derived from asteroseismic studies. The results are compared with previous estimates, with a comprehensive summary and discussion.
Methods. The basic method is similar to that previously used by the Toulouse group for solar-type stars. Models are computed with various initial chemical compositions and the computed p-mode frequencies are compared with the observed ones. All models include atomic diffusion and the importance of radiative accelerations is discussed. Several tests are used, including the usual frequency combinations and the fits of the échelle diagrams. The possible surface effects are introduced and discussed. Automatic codes are also used to find the best model for this star (SEEK, AMP) and their results are compared with that obtained with the detailed method.
Results. We find precise results for the mass, radius and age of this star, as well as its effective temperature and luminosity. We also give an estimate of the initial helium abundance. These results are important for the characterization of the star-planet system.

Key words. exoplanet-host stars – asteroseismology – stellar systems– stellar evolution

1. Introduction

In the last few years the number of observed exoplanets have increased dramatically, owing to missions like CoRoT (Baglin et al. 2006) and *Kepler* (Koch et al. 2010), as well as many other ground based and space missions (see the exoplanet encyclopedia for a complete summary [1]). Precise characterization of exoplanet host stars become more and more important in the framework of the detailed studies of the observed planetary systems. Constraints on the parameters and internal structure of the star can be obtained by comparing models with photometric and spectroscopic observations (Southworth 2011; Basu et al. 2012), but the best precision is obtained from asteroseismology, when the stellar oscillations may be observed and analysed. This was the case, for example, for the exoplanet host stars (hereafter EHS) ι Hor (Vauclair et al. 2008) and μ Arae (Soriano & Vauclair 2010), both observed with HARPS, as well as the EHS HAT-P-7, HAT-P-11 and TrES-2 (Christensen-Dalsgaard et al. 2010), observed with *Kepler*.

Among the EHS, the star HD 52265 is one of the most precisely observed for asteroseismology, as it was the only EHS observed as a main target by CoRoT. This G0V metal-rich main sequence star has an orbiting jupiter-mass planet at 0.5 AU with a period of 119 days (Naef et al. 2001; Butler et al. 2000). It was continuously observed between December 13, 2008 and March 3, 2009, that is 117 consecutive days. As a result, 31 p-mode frequencies were reported, between 1500–2550 μHz, corresponding to $\ell = 0$, 1 and 2 (Ballot et al. 2011). From this analysis, a large separation of $< \Delta\nu > = 98.4 \pm 0.1$ μHz and a small separation of $< \delta\nu_{02} > = 8.1 \pm 0.2$ μHz were found, and a complete asteroseismic analysis including mode lifetimes was presented. An extensive study of the seismic rotation of HD 52265 was performed by Stahn 2011 and Gizon et al. 2012.

Spectroscopic observations of this star were done by several groups, who gave different values of the observed triplet ([Fe/H], log g, Teff). Their results are given in Table 1. Some of these groups also observed lines of other elements, and gave detailed relative abundances. The results show an overall surmetallicity in this star, similar for most heavy elements, with a small dispersion. The Hipparcos parallax is 34.54 ± 0.40 mas (van Leeuwen 2007), which leads to a luminosity value log L/L$_\odot$ = 0.29 ± 0.05. A spectroscopic follow up was also done with the Narval spectropolarimeter installed on the Bernard Lyot telescope at Pic du Midi Observatory (France) during December 2008 and January 2009, i.e., during CoRoT observations. No magnetic signature was observed.

---

[1] http://exoplanet.eu/index.php

Preliminary modeling of this star, using spectroscopic constraints, was done by Soriano et al. (2007), as a preparation to CoRoT observations. Evolutionary tracks were computed using the Toulouse-Geneva evolution code (TGEC). According to the spectroscopic constraints, eight models with masses between 1.18 and 1.30 $M_\odot$ and metallicities ranging from 0.19 to 0.27 were chosen for further analysis, and adiabatic p-modes frequencies were computed. Echelle diagrams for each selected model were presented as well as their corresponding large and small separations. A large separation around $\sim 100\,\mu$Hz was predicted from these models except for the Takeda et al. (2005) values, which corresponded to a smaller large separation (around $\sim 75\,\mu$Hz).

The detailed CoRoT observations allow going further in this analysis, using the precise seismic results. First of all, the Takeda et al. (2005) values, which correspond to a more evolved star, are excluded. Now we present a complete asteroseismic analysis for HD 52265, and give precise results on the stellar parameters.

The method and models used for the asteroseismic comparisons with observations are described in section 2. All the models, as described in section 2.1, include element gravitational settling. The seismic tests are discussed in section 2.2 and we discuss the influence of radiative accelerations on heavy elements in section 2.3. The results are given in section 3. Section 3.1 is devoted to the results obtained without taking surface effects into account. We test the influence of varying the initial chemical composition and the introduction or not of radiative levitation on heavy elements. An analysis of surface effects and the consequences on the results is given in section 3.2. A first discussion of the results is given in section 3.3. Finally, in section 4 the results obtained using automatic codes to find the best models for this star from seismology (SEEK and AMP) are presented and compared with the previously obtained solutions. Summary and discussion are given in section 5.

Table 1. Summary of previous spectroscopic studies of HD 52265

[Fe/H]	$T_{\rm eff}$	$\log g$	Reference
0.27 ± 0.02	6162 ± 22	4.29 ± 0.04	Gonzalez et al. 2001
0.23 ± 0.05	6103 ± 52	4.28 ± 0.12	Santos et al. 2004
0.19 ± 0.03	6069 ± 15	4.12 ± 0.09	Takeda et al. 2005
0.19 ± 0.03	6076 ± 44	4.26 ± 0.06	Fischer & Valenti 2005
0.24 ± 0.02	6179 ± 18	4.36 ± 0.03	Gillon & Magain 2006
0.19 ± 0.05	6100 ± 60	4.35 ± 0.09	Ballot et al. 2011

2. Computations with TGEC

2.1. Stellar models

Stellar models were computed using the TGEC code, (Hui-Bon-Hoa 2008; Théado et al. 2012), with the OPAL equation of state and opacities (Rogers & Nayfonov 2002; Iglesias & Rogers 1996), and the NACRE nuclear reaction rates (Angulo et al. 1999). Convection was treated using the mixing length theory. For all models, the mixing length parameter was adjusted to that of the solar case, i.e. $\alpha = 1.8$ without overshooting and without extra-mixing. Gravitational settling of helium and metals was included using the Paquette prescription (Paquette et al. 1986; Michaud et al. 2004). Radiative accelerations of metals were also introduced using the SVP method (Single Valued Parameters approximation, see Alecian & LeBlanc 2002, LeBlanc & Alecian 2004 and Théado et al. 2009). As most stellar evolution codes neglect these radiative accelerations, we analysed the effects on the seismic results of introducing them or not.

Evolutionary tracks were computed for two metallicity values and two different initial helium abundances. The metallicity values were chosen as [Fe/H] = 0.23 and 0.30, so that after diffusion the final model value lies inside the observed range. Here [Fe/H] represents the global overmetallicity with respect to the Sun, defined as $[log(Z/X)_* - log(Z/X)_\odot]$, where Z and X are computed at the stellar surface. Considering the small dispersion of the detailed abundances, this value may be compared with the observed [Fe/H]. A discussion of the computed detailed abundance variations is given in section 2.3. The initial helium values are labeled as $Y_\odot$ and Y_G, where $Y_\odot$ is the solar helium value taken from Grevesse & Noels 1993 and Y_G is a helium abundance which increases with Z as expected if the local medium follows the general trend observed for the chemical evolution of galaxies (C.f. Izotov & Thuan 2004 and 2010).
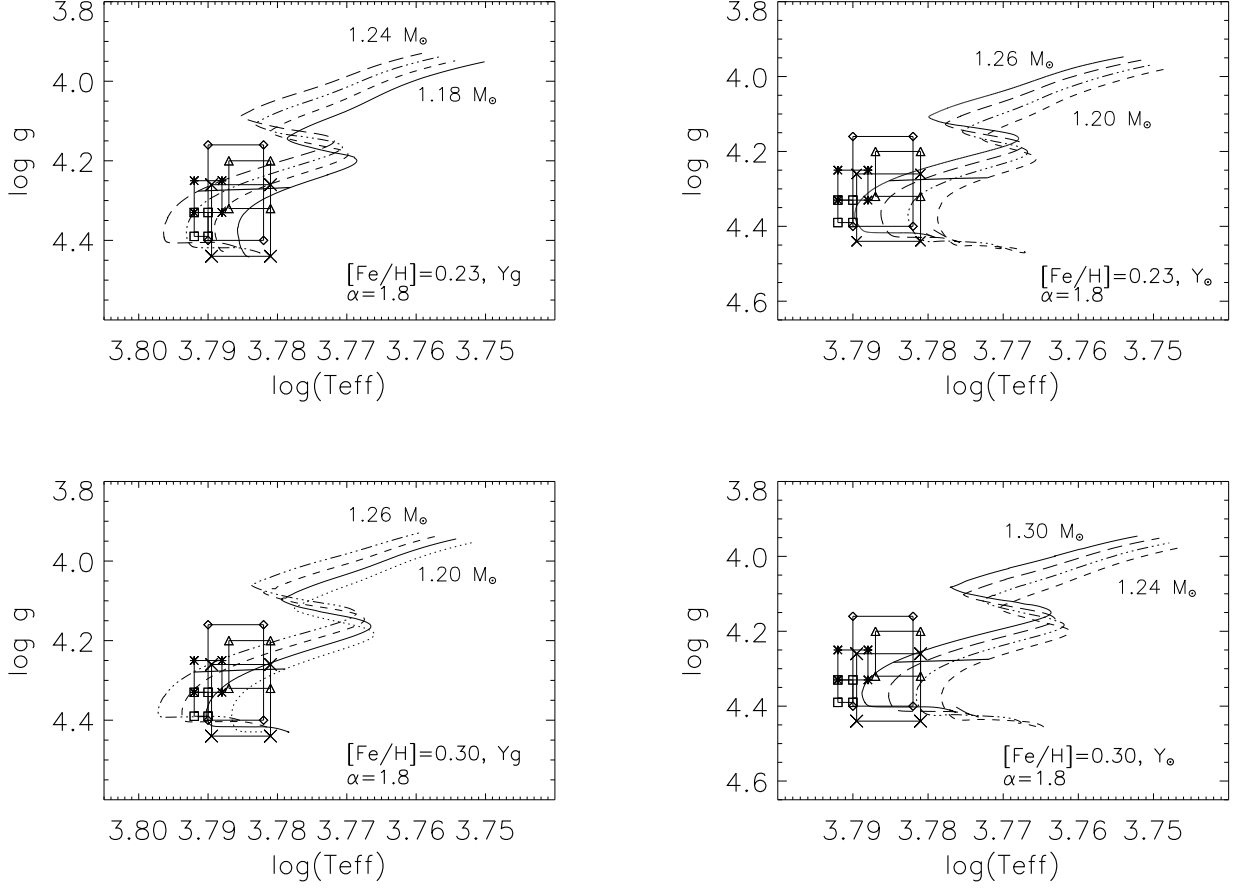
Adiabatic oscillation frequencies were computed for many models along the evolutionary tracks using the PULSE code (Brassard & Charpinet 2008). We computed these frequencies for degrees $\ell = 0$ to $\ell = 3$. For comparisons with the observations (seismic tests) we used the same frequency interval for the computed as for the observed frequencies for consistency, i.e. between 1500 and 2550 μHz, as discussed below.

2.2. Seismic Tests

A well known characteristic of p modes in spherical stars is that modes of the same degree with successive radial order n are nearly equally spaced in frequency (e.g. Tassoul 1980). The large separation is defined as:

$$\Delta\nu_{n,\ell} = \nu_{n+1,\ell} - \nu_{n,\ell} \tag{1}$$

In real stars, this large separation slightly varies with frequency, so that an average value has to be used for comparisons between models and observations. One has to be careful to use the same frequency range in both cases to do the comparisons. Taking this

Fig. 1. Evolutionary tracks in the log g vs log $T_{\rm eff}$ plane for the various sets of metallicity and helium abundance, for $\alpha = 1.8$ (see text for details). The symbols indicate the error boxes of Gonzalez et al. (2001) (*asterisks*), Santos et al. (2004) (*diamonds*), Gillon & Magain (2006) (*squares*), Fisher & Valenti (2005) (*triangles*), and Ballot et al. (2011) (*crosses*). The straight thick line represents the iso-$< \Delta\nu >$ line, with $< \Delta\nu >= 98.4\,\mu$Hz.

into account, the fit between the computed and measured large separations is the first step in the process of comparisons. The large separation gives access to the stellar average density (Ulrich 1986; White et al. 2011).

A second characteristic of p modes is that the difference between (n, ℓ) modes and $(n - 1, \ell + 2)$ ones varies very slowly with frequency. The small separations are defined as:
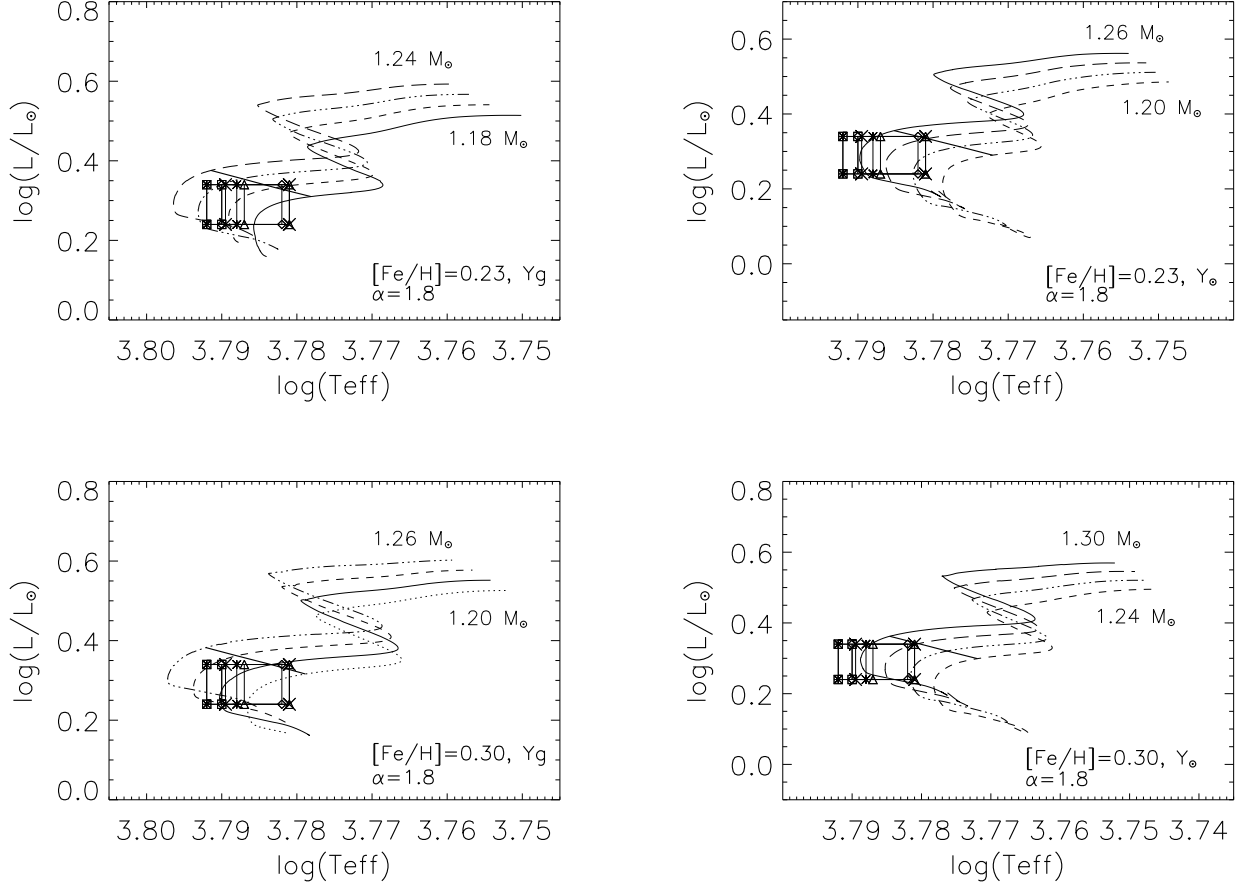
$$\delta\nu_{n,\ell} = \nu_{n,\ell} - \nu_{n-1,\ell+2} \tag{2}$$

These small separations are most sensitive to the stellar core and may give information on the extension of the convective core in some stars (Tassoul 1980; Roxburg & Vorontsov 1994; Gough 1986; Soriano & Vauclair 2008).

Provided that the stellar chemical composition is precisely known, the knowledge of both the large and the small separations, which may be plotted in the so-called C-D diagrams, gives good constraints on the stellar parameters (Christensen-Dalsgaard 1984; White et al. 2011). However, whereas the stellar metallicity can be precisely derived from spectroscopy, the helium content of solar-type stars is not directly known from observations. This ignorance leads to important uncertainties on the evolutionary tracks, and thus on the derived stellar parameters.

We analysed these uncertainties in detail by computing models with various chemical compositions. For each stellar evolutionary track that we computed, we first searched for the model which had an average large separation of $< \Delta\nu > = 98.4 \pm 0.1\,\mu$Hz. As the large separation continously decreases when the star evolves along the main sequence, one model only is found with the observed value (within the uncertainties). Then, for each set of computations done with a given initial chemical composition ([Fe/H] and Y), we looked for the model which best fitted the small separations observed between modes of $\ell = 2$ and 0, $< \delta\nu_{02} > = 8.1 \pm 0.2\,\mu$Hz. We further proceed with detailed comparisons of observed and computed échelle diagrams.

The final comparison between the models and the seismic observations needs taking into account the surface effects induced by the waves behavior in the outer stellar layers. We computed the frequency shift induced by such effects, using the recipe proposed by Kjeldsen et al. (2008). In this case, the large separations are modified, as discussed in section 3.2, which leads to corrections in the results.

Fig. 2. HR diagrams for $\alpha = 1.8$ (see text for details). Error boxes are the same horizontally as presented in Figure 1, for the effective temperatures, and correspond vertically to the luminosity uncertainty. The straight thick line represents the iso-$< \Delta\nu >$ line, with $< \Delta\nu >=98.4\,\mu$Hz.

2.3. Test on atomic diffusion: radiative accelerations

Atomic diffusion is a very important process inside stars: it can modify the atmospheric abundances and also have strong implications for the internal structure of stars (Richard, Michaud & Richer 2001; Michaud et al. 2004; Théado et al. 2009). At the present time, most stellar evolution codes include the computation of gravitational settling, but not the computation of radiative accelerations of heavy elements. These accelerations, which oppose gravitation, are negligible for the Sun but they rapidly become important for more massive stars (Michaud et al. 1976). The variations with depth of the radiative accelerations on specific elements can lead to their accumulation or depletion in various layers inside stars. The presence of a heavy iron layer above layers with smaller molecular weights creates an inverse μ-gradient, unstable towards thermohaline convection (Vauclair 2004). This induced mixing has also to be taken into account in computations of stellar modeling (Théado et al. 2009). An improved TGEC version including radiative accelerations on C, N, O, Ca and Fe was recently developped (Théado et al. 2012). This new version was used to compare the oscillation frequencies computed with and without introducing the radiative accelerations in the models. We found that, for solar-type stars (masses less than 1.30 M$_\odot$), the difference in the computed frequencies is small. Two models with the same mass of 1.28 M$_\odot$ and the same average large separations of 98.26 μHz, one computed with the radiative accelerations and one neglecting them, present differences in the average small separations of the order of 0.01 μHz. These differences between the two models decrease with decreasing stellar mass. We conclude that the radiative accelerations may be neglected in the following computations.

The result that radiative accelerations have no important consequences in the present models is consistent with the fact that the detailed abundances do not show large relative variations for the observed elements (Section 1). Indeed, in case of gravitational settling, the abundances of heavy elements all decrease in a similar way, in spite of their different masses, due to the slowing down effect of the coulomb forces. The diffusion velocities vary typically as A/Z^2 where A is the mass number and Z the charge, which is similar for various elements in stellar conditions. This behavior would be modified if radiative accelerations were important.

Table 2. Examples of models with α=1.8, without surface effects.

[Fe/H]$_i$	Y$_i$	M/M$_\odot$	Age [Gyr]	[Fe/H]$_S$	Y$_S$	log g	log T_{eff} [K]	log $(L/L_\odot)$	R/R$_\odot$	M/R^3 [solar units]	$< \Delta\nu >$ [μHz]	$< \delta\nu_{02} >$ [μHz]
0.23	0.293	1.18	3.682	0.16	0.246	4.267	3.778	0.310	1.328	0.50	98.31	7.08
0.23	0.293	1.20	3.204	0.16	0.246	4.271	3.782	0.332	1.333	0.51	98.38	7.54
0.23	0.293	1.22	2.820	0.16	0.248	4.273	3.787	0.355	1.341	0.51	98.36	7.85
0.23	0.293	1.24	2.416	0.15	0.242	4.276	3.791	0.375	1.347	0.51	98.34	8.33
0.23	0.271	1.22	3.756	0.16	0.228	4.272	3.776	0.312	1.343	0.51	98.33	7.11
0.23	0.271	1.24	3.283	0.16	0.228	4.275	3.780	0.334	1.349	0.51	98.31	7.80
0.23	0.271	1.26	2.865	0.16	0.230	4.278	3.785	0.355	1.355	0.51	98.34	7.98
0.23	0.271	1.28	2.461	0.16	0.227	4.281	3.789	0.375	1.361	0.51	98.35	8.30
0.30	0.303	1.20	3.209	0.23	0.257	4.271	3.778	0.316	1.333	0.51	98.42	7.35
0.30	0.303	1.22	2.820	0.23	0.258	4.273	3.783	0.339	1.341	0.51	98.35	7.75
0.30	0.303	1.24	2.431	0.23	0.261	4.276	3.787	0.361	1.347	0.51	98.38	8.11
0.30	0.303	1.26	2.072	0.22	0.254	4.282	3.792	0.382	1.354	0.51	98.38	8.59
0.30	0.271	1.24	3.771	0.23	0.231	4.274	3.771	0.299	1.349	0.51	98.32	7.11
0.30	0.271	1.26	3.293	0.23	0.231	4.277	3.776	0.320	1.356	0.51	98.37	7.64
0.30	0.271	1.28	2.865	0.23	0.231	4.280	3.780	0.341	1.363	0.51	98.34	7.87
0.30	0.271	1.30	2.476	0.24	0.233	4.282	3.784	0.362	1.369	0.51	98.39	8.25

Table 3. Examples of models with α=1.8 , including surface effects. Here $< \Delta\nu^* >$ represents the Kjeldsen et al. (2008)-corrected large separations.

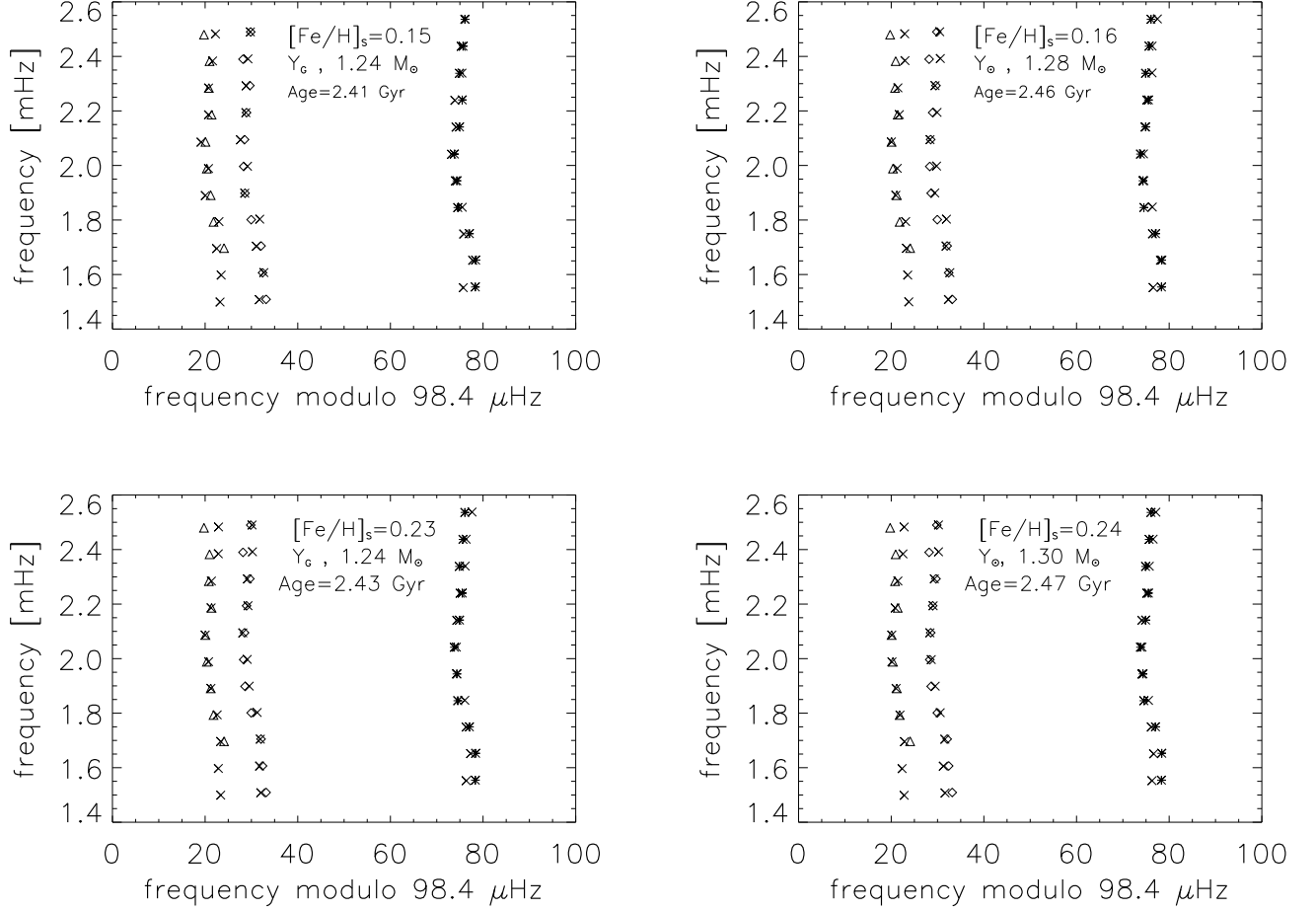| [Fe/H]$_i$	Y$_i$	M/M$_\odot$	Age [Gyr]	[Fe/H]$_S$	Y$_S$	log g	log T_{eff} [K]	log $(L/L_\odot)$	R/R$_\odot$	M/R^3 [solar units]	$< \Delta\nu^* >$ [μHz]	$< \Delta\nu >$ [μHz]	$< \delta\nu_{02} >$ [μHz]
0.23	0.293	1.18	3.548	0.16	0.247	4.275	3.779	0.306	1.315	0.52	99.67	98.27	7.27
0.23	0.293	1.20	3.069	0.16	0.247	4.279	3.784	0.328	1.321	0.52	99.68	98.27	7.83
0.23	0.293	1.22	2.670	0.16	0.250	4.282	3.788	0.350	1.327	0.52	99.86	98.19	8.11
0.23	0.293	1.24	2.251	0.16	0.244	4.287	3.792	0.369	1.331	0.52	100.08	98.19	8.47
0.23	0.271	1.20	4.130	0.16	0.228	4.276	3.773	0.287	1.325	0.52	99.51	98.19	6.85
0.23	0.271	1.22	3.622	0.16	0.228	4.279	3.777	0.309	1.331	0.52	99.56	98.18	7.26
0.23	0.271	1.24	3.149	0.16	0.229	4.283	3.781	0.330	1.337	0.52	99.61	98.18	7.69
0.23	0.271	1.26	2.730	0.16	0.232	4.286	3.786	0.351	1.343	0.52	99.62	98.07	8.11
0.30	0.303	1.20	3.089	0.23	0.258	4.278	3.780	0.313	1.322	0.52	99.64	98.32	7.70
0.30	0.303	1.22	2.685	0.23	0.260	4.282	3.784	0.335	1.328	0.52	99.72	98.13	7.94
0.30	0.303	1.24	2.296	0.24	0.263	4.285	3.788	0.357	1.334	0.52	99.78	98.15	8.34
0.30	0.303	1.26	1.907	0.23	0.257	4.290	3.793	0.376	1.337	0.52	100.23	98.20	8.84
0.30	0.271	1.24	3.637	0.23	0.231	4.282	3.773	0.295	1.338	0.52	99.56	98.27	7.30
0.30	0.271	1.26	3.173	0.23	0.232	4.284	3.777	0.317	1.345	0.52	99.50	98.16	7.64
0.30	0.271	1.28	2.730	0.23	0.233	4.288	3.781	0.337	1.351	0.52	99.64	98.09	8.08
0.30	0.271	1.30	2.326	0.23	0.236	4.291	3.785	0.357	1.355	0.52	99.80	98.20	8.52

3. Results

3.1. Computations without surface effects

The computations of evolutionary tracks, with two initial metallicity values, [Fe/H] = 0.23 and 0.30, and two different helium abundances, Y$_\odot$ equal to 0.271 and Y$_G$ respectively equal to 0.293 and 0.303 for the two metallicity values, lead to four different sets of tracks, each of them covering a mass range from 1.10 to 1.30 $M_\odot$. A few of these tracks are presented in Figures 1 and 2. Error boxes of five of the spectroscopic studies given in Table 1 are also drawn in these figures.

As explained in previous sections, we found, along each evolutionary track, a model which has an average large separation consistent with the observed one, computed in the same frequency range, of $\sim$ [1.5, 2.5] mHz. The location of all these models in the log g - log T_{eff} plane as well as in the HR diagrams are indicated in Figures 1 and 2 with iso-$< \Delta\nu > 98.4$ μHz lines. For each case, we also computed the average small separation, $\delta\nu_{n,02}$ (Table 2). We can see that for models with the same large separation, the small separation increases for increasing mass, so that in each case (i.e. for each set of chemical composition), there is a model that is consistent with both the large and small separations. However, when comparing the absolute model frequencies with the observed ones, we find that we must shift the computed frequencies by about 20 μHz to obtain the best fit with the observed ones. This offset is attributed to surface effects. The échelle diagrams corresponding to these best models are given in Figure 3.

3.2. Computations including surface effects

We know that stellar modeling fails to represent properly the near-surface layers of the stars. As a consequence, there is a systematic offset between observed and computed frequencies. This offset is independent of the angular degree ℓ and increases with frequency.

Fig. 3. Echelle diagrams for the best model found for each set of evolutionary tracks calculated with $\alpha = 1.8$. In this set of models, the surface effects are not included. The model frequencies (*crosses*) are compared to the observed frequencies, represented as diamonds (ℓ=0), asterisks (ℓ=1), and triangles (ℓ=2).To obtain these best fits we had to shift the model frequencies by respectively (top left, top right, bottom left, bottom right) 27, 25, 24, 22 μHz (see text)

This has been studied in the case of the Sun, and a similar offset is expected to occur in other stars. Using the Sun as a reference, Kjeldsen et al. (2008) suggested that for other stars, the near-surface correction on the frequencies may be approximated by:
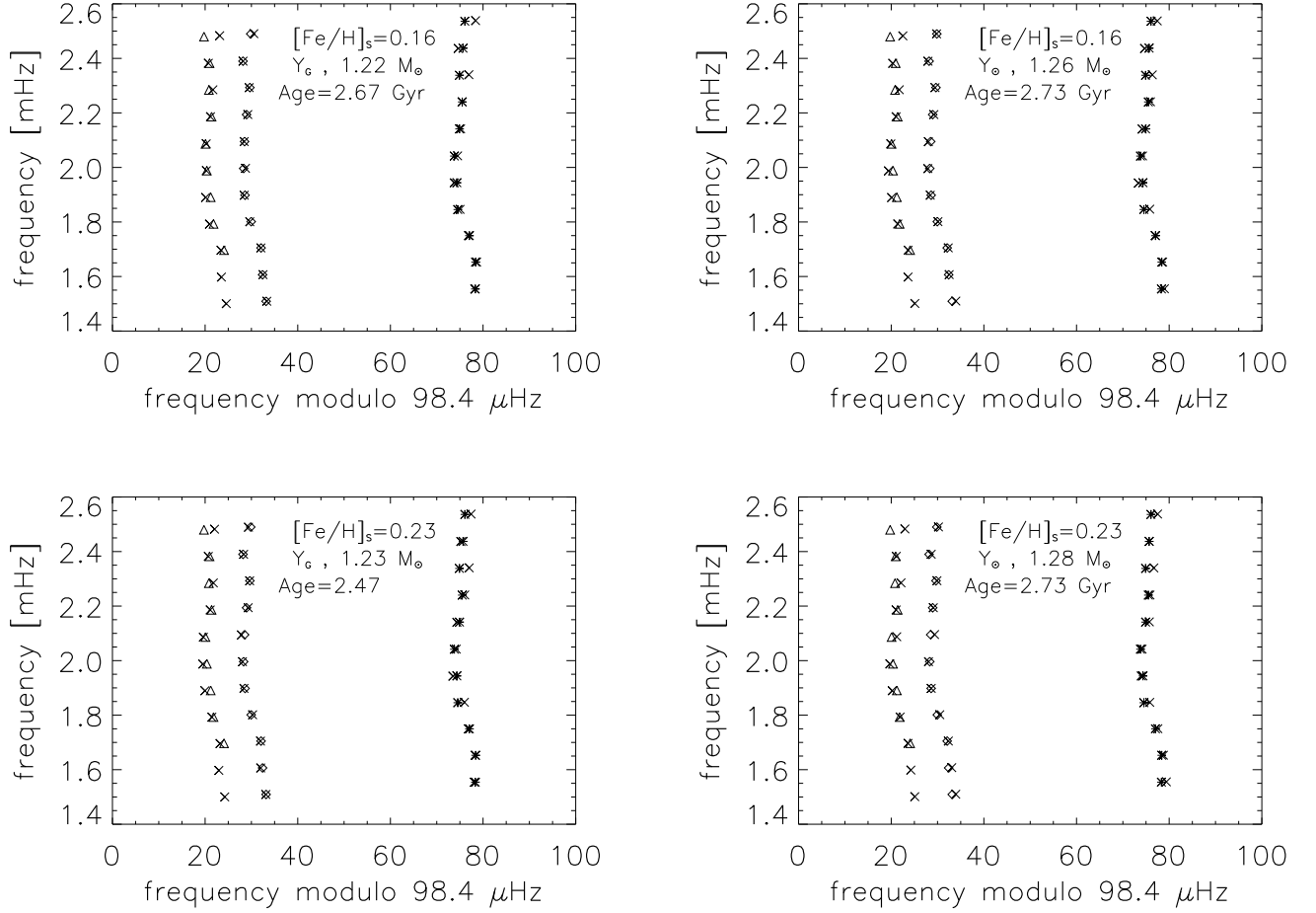
$$\nu_{\text{obs}}(n) - \nu_{\text{best}}(n) = a \left[\frac{\nu_{\text{obs}}(n)}{\nu_0} \right]^b \tag{3}$$

where $\nu_{\text{obs}}(n)$ are the observed ℓ=0 frequencies with radial order n, $\nu_{\text{best}}(n)$ are the calculated frequencies for the best model which is the model that best describes the star but which still fails to model correctly the near-surface layers, and ν_0 is a constant reference frequency, chosen to be that of the frequency at the maximum amplitude in the power spectrum. The parameter a may be derived as a function of the parameter b, which has to be adjusted to the solar case. We used this method to find the frequency corrections that we have to apply to our models, which lead to a new average large separation $< \Delta\nu^* >$, slightly larger than the observed one. We then proceed as before to derive models for the same sets of values of the helium abundance and metallicity, using $\alpha = 1.8$ (Table 3). Figure 4 presents échelle diagrams obtained with the new best models. In these graphs, the frequency corrections have been applied to the new model frequencies in order to compare them directly with the observations.

3.3. Best models and discussion

We give in Table 4 the parameters of the best models that we obtained for the four different sets of chemical composition. These models have been computed with a mixing length parameter of 1.8, the frequencies have been corrected for surface effects and the computed large and small separations are the closest to the observed ones in the sample. We also give the χ^2 values for the comparisons of the three ℓ = 0, 1, 2 lines in the échelle diagrams.

Figure 5 displays the large and small separations as a function of the frequency for the observations and the four best models. The pattern observed in the large separations are well reproduced by the models. For the small separations, the agreement is also

Fig. 4. Echelle diagrams for the best model, including near-surface corrections, as proposed by Kjeldsen et al. 2008 found for each set of evolutionary tracks calculated with $\alpha = 1.8$, in comparison with observed frequencies. The symbols are the same ones as in Figure 3.
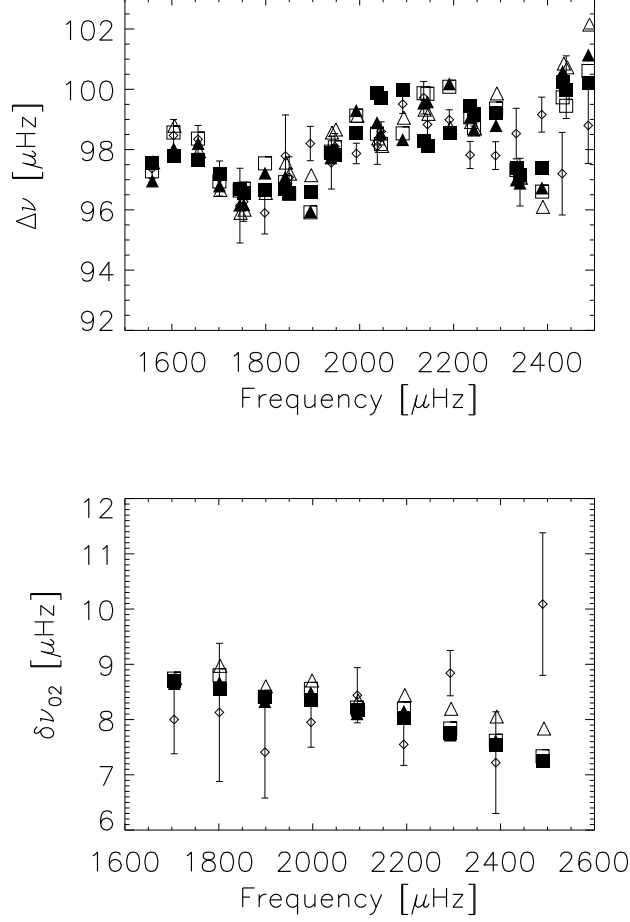
Table 4. Best models obtained with the TGEC code, including near surface corrections.

$M/M_\odot$	$L/L_\odot$	$R/R_\odot$	$\log g$	$T_{\rm eff}$ [K]	age [Gyr]	$[Fe/H]_i$	Y_i	$[Fe/H]_S$	Y_S	χ^2
1.22	2.239	1.327	4.282	6143	2.670	0.23	0.293	0.16	0.250	5.06
1.23	2.219	1.330	4.283	6120	2.476	0.30	0.303	0.23	0.262	3.34
1.26	2.244	1.343	4.286	6109	2.730	0.23	0.271	0.16	0.232	6.42
1.28	2.173	1.351	4.288	6043	2.730	0.30	0.271	0.23	0.233	3.51

very good except for two points at large frequencies (2284 μHz and 2479 μHz). This suggests that the uncertainties given in Ballot et al. (2011) for these points were underestimated.

Several concluding points can already be derived from a first analysis of Table 4. First of all, the stellar gravity is obtained, as usual, with a precision of order 0.1%. The mass and age depend basically on the chosen value for the initial helium content. For a low helium value, the mass is 1.26 to 1.28 $M_\odot$, and the age 2.73 Gyr, whereas for a larger helium value the mass is slightly smaller (around 1.22 - 1.23 $M_\odot$) as well as the age (2.48 to 2.68 Gyr). In any case the radius and luminosity are known with a precision of order 1%.

We can go further by comparing the effective temperatures of the models with the spectroscopic observations (Figure 6). As found before for the cases of ι Hor (Vauclair et al. 2008) and μ Arae (Soriano & Vauclair 2010), the effective temperatures of the best models are smaller for smaller initial helium and larger for smaller metallicity. In the present case, we find that the model with the largest metallicity and the smallest helium, represented by black square in figure 6, is at the coolest limit of the observational boxes and thus may be excluded from the sample on spectroscopic considerations. We derive the stellar parameters from a mean value of the resulting three models, as given in Table 5.

Fig. 5. Comparisons between the large separations (top) and the small separations (bottom) of the four best models indicated by squares for models with [Fe/H]$_s$=0.23 ([Fe/H]$_i$=0.30) and triangles for models with [Fe/H]$_s$=0.16 ([Fe/H]$_i$=0.23). Empty symbols are used to indicated an helium abundance according to Y$_g$, and filled symbols for a solar helium abundance (see text for details.) Observations are represented as white diamonds.

4. Scaling relations and automatic fits

4.1. Scaling relations

The empirical scaling relations proposed by Kjeldsen & Bedding (1995) can give approximate values of the mass and radius of a star from the observed average large separation, the frequency at the maximum of the power spectrum and the observed effective temperature:

$$\frac{M}{M_\odot} = \left(\frac{135\mu Hz}{<\Delta\nu>}\right)^4 \left(\frac{\nu_{max}}{3050\mu Hz}\right)^3 \left(\frac{T_{eff}}{5777K}\right)^{3/2} \tag{4}$$

$$\frac{R}{R_\odot} = \left(\frac{135\mu Hz}{<\Delta\nu>}\right)^2 \left(\frac{\nu_{max}}{3050\mu Hz}\right) \left(\frac{T_{eff}}{5777K}\right)^{1/2} \tag{5}$$

For HD 52265, the frequency at the maximum amplitude is ν_{max} = 2090 ± 20 μHz (Ballot et al. 2011). With a large separation of 98.4 μHz and an effective temperature of 6100 K, we obtain from these relations M = 1.23$M_\odot$ and R = 1.32$R_\odot$. With a large separation corrected for the surface effects, of 99.4 μHz, we obtain M = 1.19$M_\odot$ and R = 1.29$R_\odot$. In spite of the uncertainties, these results are in good agreement with our own results.

4.2. Results from the SEEK code

Computations have been done for this star using the SEEK automatic code (Quirion et al. 2010, and Gizon et al. 2012). This code makes use of a large grid of stellar models computed with the Aarhus Stellar Evolution Code (ASTEC). It searches for the best model corresponding to a seismically observed star, with the help of Bayesian statistics. The input parameters are the large and small

Fig. 6. Location of the best models in the log g vs log T_{eff} plane. Triangles indicate models with [Fe/H]$_s$=0.16 ([Fe/H]$_i$=0.23), and squares indicate models with [Fe/H]$_s$=0.23 ([Fe/H]$_i$=0.30). Filled symbols are used to show the models with a solar helium value. Error boxes correspond to Gonzalez et al. (2001) (*asterisks*), Santos et al. (2004) (*diamonds*), Gillon & Magain (2006) (*squares*), Fisher & Valenti (2005) (*triangles*), and Ballot et al. (2011) (*crosses*) spectroscopic studies.

average separations, the spectroscopic observables (T$_{eff}$, log g, [Fe/H]) and the absolute magnitude. The output gives the stellar mass, the radius and the age. In the case of HD 52265 the values given by the SEEK code for the mass and radius are slightly larger than our results, and the age is smaller : $M = 1.27 \pm 0.03 M_\odot$, $R = 1.34 \pm 0.02 R_\odot$ and age = 2.37 ± 0.29 Gyr. The difference between the SEEK results and ours may be related to a different initial helium, to slightly different values of the average large and small separations as given by Gizon et al. (2012), or to the fact that the SEEK results correspond to a secondary maximum of probability, as discussed below.

4.3. Results from the Asteroseismic Modeling Portal

We also performed computations for HD 52265 using the Asteroseismic Modeling Portal (https://amp.ucar.edu/). The AMP provides a web-based interface for deriving stellar parameters for Sun-like stars from asteroseismic data. AMP was developed at the High Altitude Observatory and the Computational & Information Systems Laboratory of the National Center for Atmospheric Research (Metcalfe et al. 2009). It uses the ASTEC and ADIPLS codes (Christensen-Dalsgaard 2008 a,b) coupled with a parallel genetic algorithm (Metcalfe & Charbonneau 2003). Two different computations were done, the first one, AMP(a), by S. Vauclair using all the observed frequencies as given by Ballot et al. (2011), and the second one, AMP(b), by S. Mathur using only the most reliable frequencies ((l=0, n=14), (l=1, n=14) and (l=2,n=15) were excluded). The final results are very close to the parameters found by using the TGEC code (Table 6). Interestingly enough, the code found also solutions for a mass of 1.27 $M_\odot$ with a small Y (about 0.26) and a small age (about 2.7 Gyr) but the χ^2 tests showed that these results corresponded to secondary maxima, not to the best solution.

Table 5. Final results for the parameters of the exoplanet-host star HD 52265 obtained with the TGEC code.

M/M$_\odot$ = 1.24 ± 0.02	$[Fe/H]_i$ = 0.27 ± 0.04
R/R$_\odot$ = 1.33 ± 0.02	Y_i = 0.28 ± 0.02
L/L$_\odot$ = 2.23 ± 0.03	$[Fe/H]_s$ = 0.20 ± 0.04
log g = 4.284 ± 0.002	Y_s = 0.25 ± 0.02
Age (Gyr) = 2.6 ± 0.2	T_{eff} (K) = 6120 ± 20

5. Summary and Conclusions

In the present paper, we performed a detailed analysis of the exoplanet-host star HD 52265, which has been observed by CoRoT during 117 consecutive days, as one of the main targets. The beautiful observational results obtained for this star (Ballot et al. 2011) allowed a precise determination of its parameters, using classical comparisons between models computed with the TGEC and observational data. In our computations, we included atomic diffusion of helium and heavy elements. We found that, for the computed stellar models, the effects of radiative accelerations on individual elements is small and may be neglected. This result is consistent with the fact that detailed abundance analysis show similar enhancements in heavy elements compared to the Sun. We iterated the model computations so as to find a final surface [Fe/H]$_s$ in the observational range. We also compared these results with those obtained using approximate scaling relations (Kjeldsen & Bedding 1995), and automatic codes like SEEK (Quirion et al.

Table 6. Final results for the parameters of the exoplanet-host star HD 52265 obtained from AMP automatic analysis, using all observed frequencies (a) or only the most reliable frequencies (b).

	AMP(a)	AMP(b)
$M/M_\odot$	1.22	1.20
$R/R_\odot$	1.321	1.310
$L/L_\odot$	2.058	2.128
log g	4.282	4.282
$[Fe/H]$	0.23	0.215
Y	0.280	0.298
Age (Gyr)	3.00	2.38
T_{eff}	6019	6097

2010) and AMP (Metcalfe et al. 2009). Although the detailed physics included in the models is different, these results are in good agreement.

The good concordance between the results obtained with the TGEC code and the AMP for Sun-like stars was already proved with the star μ Arae. The results for this star, which were published separately (Soriano & Vauclair 2010 for TGEC; Doğan et al. 2012 for AMP), are presented in the appendix for comparison. Altogether, these works represent real success of the asteroseismic studies for Sun-like stars.

References

Alecian, G., LeBlanc, F., 2002, MNRAS, 332, 891
Angulo, C., Arnould, M., Rayer, M., et al. 1999, Nuclear Physics A, 656, 3 http://pntpm.ylb.ac.be/Nacre/nacre.htm
Baglin, A., Auvergne, M., Barge, P., et al. 2006, in ESA Special Publication, Vol. 1306, The CoRoT Mission: Pre-launch Status, ed. M. Fridlund, A. Baglin, J. Lochard, & L. Conroy (ESA Publication Divisions, Noordwijk), 33
Basu, S., Verner, G.A., Chaplin, W.J.,& Elsworth, Y., 2012, ApJ 746, 76
Ballot, J., Gizon, L., Samadi, R., et al. 2011, A&A, 530, 97
Brassard, P., & Charpinet, S. 2008, Ap&SS, 316, 107
Butler, R. P., Vogt, S., Marcy, G., et al. 2000, ApJ 545, 504
Christensen-Dalsgaard, J., 1984, in Space Research in Stellar and Variability, ed. A. Mangeney & F. Praderie, 11
Christensen-Dalsgaard, J., Kjeldsen, H., Brown, T. M., et al. 2010, ApJ, 713, L164
Christensen-Dalsgaard, J.,2008a, Ap&SS, 316, 13
Christensen-Dalsgaard, J.,2008b, Ap&SS, 316, 113
Doğan, G., Metcalfe, T.S., Woitaszek, M., et al. 2012, submitted to Ap.J.
Fischer, D. A., & Valenti, J. A. 2005, ApJ, 622, 1102
Gillon, M., & Magain, P. 2006, A&A, 448, 341
Gizon, L., Ballot, J., Michel, E. et al. 2012, submitted to Nature
Gonzalez, G., Laws, C., Tyagi, S., & Reddy, B. E. 2001, ApJ, 121, 432
Gough, D. O. 1986, in Hydrodynamic and magnetohydrodynamic problems in the Sun and stars, ed. Y. Osaki (Uni. of Tokyo Press), 117
Grevesse, N., & Noels, A. 1993, in Origin and Evolution of the Elements, ed. Prantzos, N., Vangioni-Flam, E., & Cassé, M., Cambridge University Press, 15
Hui-Bon-Hoa, A. 2008, Ap&SS, 316, 55H
Iglesias, C. A., & Rogers, F. J. 1996, ApJ, 464, 943
Izotov, Y. I., & Thuan, T. X. 2004, ApJ, 602, 200
Izotov, Y. I., & Thuan, T. X. 2010, ApJ, 710, L67
Kjeldsen, H.,& Bedding, T. R.,1995, A&A, 293, 87
Kjeldsen, H., Bedding, T. R., & Christensen-Dalsgaard, J. 2008, ApJ, 683, L175
Koch, D. G., Borucki, W. J., Basri, G., et al. 2010, ApJ, 713, L79
LeBlanc, F., Alecian, G., 2004, MNRAS, 352, 1329L
van Leeuwen, F., 2007, A& A, 474, 653
Metcalfe, T., Creevey, O.L.,& Christensen-Dalsgaard, J. 2009, ApJ, 699, 373
Metcalfe, T., Charbonneau, P., 2003, JCoPh, 185, 176
Michaud, G., Charland, Y., Vauclair, S., Vauclair, G., 1976, ApJ, 210, 447
Michaud, G., Richard, O.,Richer, J., & VandenBerg, D. 2004, ApJ, 606, 452
Naef, D., Mayor, M., Pepe, F., et al. 2001, A&A, 375, 205
Paquette, C., Pelletier, C., Fontaine, G., & Michaud, G. 1986, ApJS, 61, 177
Quirion, P.O., Christensen-Dalsgaard, J., & Arenthoft, T., 2010, ApJ 725, 2176
Richard, O., Michaud, G., Richer, J., 2001, ApJ, 558, 377
Rogers, F. J., & Nayfonov, A. 2002, ApJ, 576, 1064
Roxburgh, I. W., & Vorontsov, S. V. 1994, MNRAS, 267, 297
Santos, N. C., Israelian, G., & Mayor, M. 2004, A&A, 415, 1153
Soriano, M., Vauclair, S., Vauclair, G., & Laymand, M. 2007, A&A, 471, 885
Soriano, M., & Vauclair, S. 2008, A&A, 488, 975
Soriano, M., & Vauclair, S. 2010, A&A, 513, A49
Southworth, J., 2011, MNRAS, 417, 216
Stahn, T., 2011, PhD thesis, University of Göttingen, Germany
Takeda, Y., Ohkubo, M., Sato, B., Kambe, E., & Sadakane, K. 2005, PASJ, 57, 27
Tassoul, M., 1980, ApJS, 43, 469
Théado, S., Vauclair, S., Alecian, G., & LeBlanc, F. 2009, ApJ, 704, 1262

Théado, S., Alecian, G., LeBlanc, F., & Vauclair, S., 2012, in preparation
Ulrich, R.K., 1986, ApJ, 306, L37
Vauclair, S. 2004, ApJ, 605, 874
Vauclair, S., Laymand, M., Bouchy, F. et al. 2008, A&A, 482, L5
White, T.R., Bedding, T.R., Stello, D., Christensen-Dalsgaard, J., Huber, D, & Kjeldsen, H., ApJ, 743, 161

Appendix A:

Comparison of the results given by the TGEC analysis (Soriano & Vauclair 2008) and the Asteroseismic Modeling Portal (Doğan et al.2012) for the exoplanet-host sun-like star μ Arae.

Table A.1. Comparison of the results obtained with the TGEC and the Asteroseismic Modeling Portail for μ Arae.

	TGEC	AMP
$M/M_\odot$	1.1 ± 0.02	1.1
$R/R_\odot$	1.36 ± 0.06	1.365
$L/L_\odot$	1.90 ± 0.10	1.894
log g	4.215 ± 0.005	4.213
T_{eff}	5820 ± 50	5807
$[Fe/H]$	$+0.32 \pm 0.02$	+0.418
Y	0.30 ± 0.01	0.316
age(Gyr)	6.34 ± 0.80	6.66